PTEP

Prog. Theor. Exp. Phys. **2019**, 053C01 (14 pages)
DOI: 10.1093/ptep/ptz040

Imaging the inner structure of a nuclear reactor by cosmic muon radiography

Hirofumi Fujii[1], Kazuhiko Hara[2], Shogo Hashimoto[2,5], Kohei Hayashi[1], Fumiaki Ito[2], Hidekazu Kakuno[3], Hideyo Kodama[1], Kanetada Nagamine[1], Kazuyuki Sato[2,6], Kotaro Satoh[1], Shin-Hong Kim[2], Atsuto Suzuki[1,7], Takayuki Sumiyoshi[3], Kazuki Takahashi[2,5], Yu Takahashi[2,8], Fumihiko Takasaki[1,*], Shuji Tanaka[1], and Satoru Yamashita[4]

[1]*High Energy Accelerator Research Organization (KEK), Tsukuba, Ibaraki 305-0801, Japan*
[2]*University of Tsukuba, Tsukuba, Ibaraki 305-8571, Japan*
[3]*Tokyo Metropolitan University, Japan*
[4]*University of Tokyo, Japan*
[5]*Present address: NEDO*
[6]*Present address: Iwate Prefectural University*
[7]*Present address: JAEA*
[8]*Present address: JAXA*
*E-mail: fumihiko.takasaki@kek.jp

Received October 17, 2018; Revised January 14, 2019; Accepted January 24, 2019; Published May 24, 2019

We studied the inner structure of the nuclear reactor of the Japan Atomic Power Company (JAPC) at Tokai, Japan, by muon radiography. Muon detectors were placed outside the reactor building. By detecting cosmic muons penetrating the wall of the reactor building, we could successfully identify objects such as the containment vessel, pressure vessel, and other structures of the reactor. We also observed a concentration of heavy material which can be attributed to the nuclear fuel assemblies stored in the nuclear fuel storage pool.

Subject Index C50

1. Introduction

The nuclear power reactors at Fukushima Daiichi, Japan, were seriously damaged by the gigantic earthquake and tsunami in March, 2011. Decommissioning of the damaged reactors is necessary, and establishing the procedure of decommissioning is one of the urgent tasks. As the reactor buildings and their surrounding area are highly radioactive, close inspection of the reactors is very difficult. It has been proposed to use cosmic muons to diagnose the reactor status from outside the reactor building by cosmic muon radiography [1,2], measuring the millions of cosmic muons which penetrate the reactor and thus figuring out the detailed structure of the reactor. Cosmic muon detectors are placed outside the damaged reactor building; from the observed muon distribution, it was hoped to visualize the inner structure of the reactors.

In order to demonstrate the usefulness of the cosmic muon radiography technology in visualizing the inner structure of the reactor, we measured the cosmic muons penetrating the nuclear reactor of the Japan Atomic Power Company (JAPC), Tokai, Ibaraki, Japan. A picture of the investigated JAPC reactor building is shown in Fig. 1. The main building is about 40 m high and 40 m wide. This reactor is a GM MKII type and its conceptual structure is shown in Fig. 2. The measurements were made

Fig. 1. The investigated nuclear power reactor of JAPC at Tokai (courtesy of JAPC).

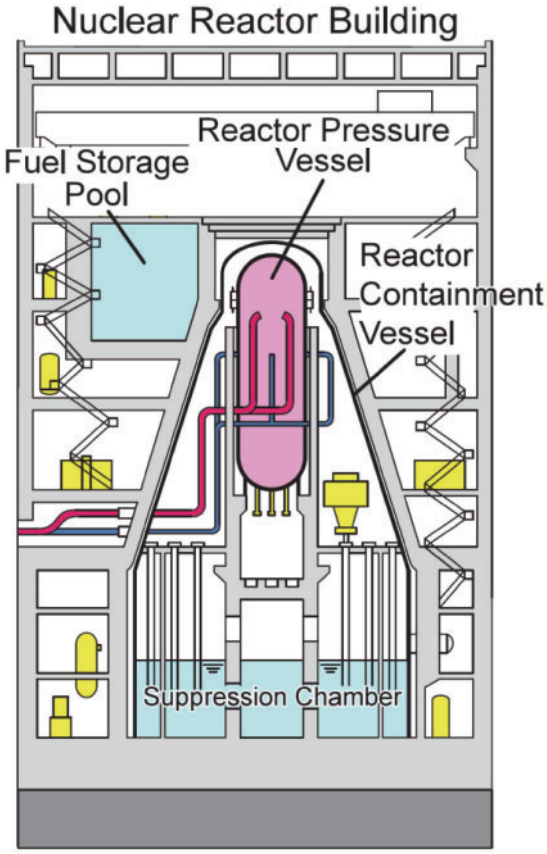

Fig. 2. Conceptual image of the reactor structure at JAPC, Tokai.

from February 2012 to December 2013. During this period, the reactor ceased generating electricity and nuclear fuels were taken out and stored in the storage water pool (NFSP). We reported the results of our first measurement in Ref. [3], concluding that (i) no fuel was loaded in the reactor and (ii) a cluster of heavy objects was identified at the location of the NFSP. Since February 2013 we have added a second system at a horizontal viewing angle of nearly 90° with respect to the first system. This report describes the impact of this addition: we succeeded in 3D imaging of the cluster of fuel objects placed in the NFSP.

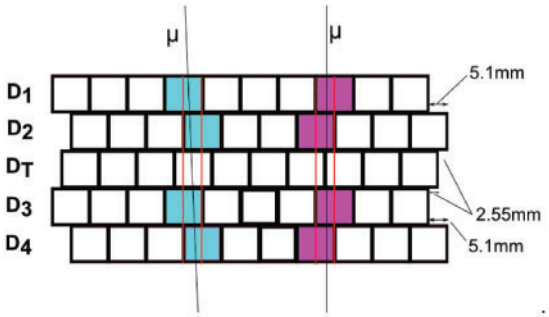

Fig. 3. Cross sectional view of the PSC arrangement of the test detector system. The PSCs in the layer marked as D_T are used to estimate the detection efficiency. Two cases are shown: Case 1 (blue): muons traversing through the center of a PSC in the D_T layer; Case 2 (purple): muons traversing the boundary regions of adjacent PSCs.

2. The muon detection system

Since the details of the muon detection system are given in Ref. [3], we briefly describe here the detection system supplementing the previous description. The major difference is the addition of the second muon telescope, made of two X–Y units of plastic scintillation counters (PSC). The two X–Y units are separated by 1. 5 m. We call this telescope MT2. It is not equipped with a magnet, unlike MT1 [3] of the first muon telescope system.

The basic unit of the PSC is composed of a scintillator bar of 1 m length and 1×1 cm^2 in cross section with an extruded hole at the center [4], where a 1 mmϕgavelength-shifter fiber [5] is embedded. One end of the fiber is coupled with a multi-pixel photon counter (MPPC) [6]. The efficiency of the PSC was evaluated [7] using cosmic muons in a test detector system fabricated using the same PSCs. The test detector system has a five-layer structure with 10 PSCs assembled in each layer, as shown in Fig. 3. We evaluated the detection efficiency of a particular PSC in the middle layer D_T while the traversing muon track was identified by the PSCs colored blue in the D_1, D_2, D_3 and D_4 layers.

We counted the number of events, N_1, with the condition of having coincident signals from the blue-colored PSCs, and the number of events, N_2, requiring an additional coincident signal from the PSC in the D_T layer. The detection efficiency for cosmic muons was estimated from the ratio N_2/N_1 by changing the threshold voltage to the D_T layer. As can be seen in Fig. 4, the detection efficiency of the PSC approaches unity for small values of the threshold V_{th} and drops to almost zero for V_{th} higher than 1 V. A similar study was made for the case where the muon traverses the gap region of the plane (see Fig. 3). Taking into account the gaps between the PSCs, the overall detection efficiency for the muons of normal entry is estimated to be better than 95%. The efficiency is expected to be better for muons traversing at angles.

3. Imaging the reactor at JAPC, Tokai

3.1. Location of the muon telescopes

The previous results in Ref. [3] were obtained with one muon telescope, MT1, placed 63 m away from the reactor center at the location MT1-1 shown in Fig. 5.

We continued the observation by slightly changing the location of MT1 to MT1-2 and by deploying another telescope, MT2. The locations were chosen in consultation with JAPC. The telescope MT1 was placed on the ground outside the reactor building 61–63 m away from the reactor center. MT1-1 was directed at the center of the pressure vessel, where the nuclear fuel is loaded when the reactor is

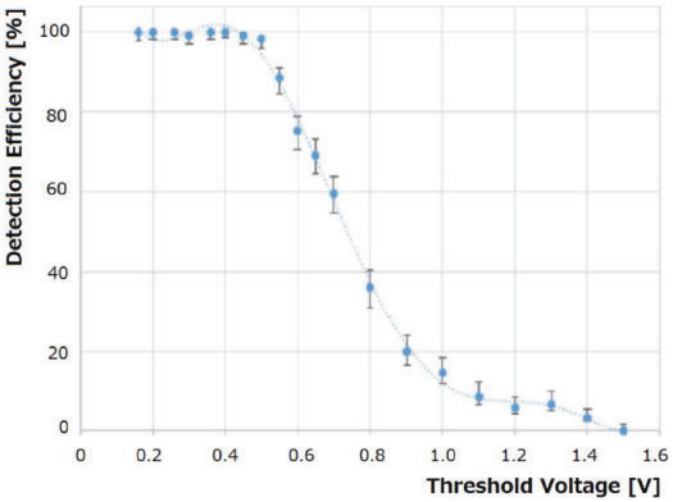

Fig. 4. Detection efficiency of the muon detector for cosmic muons as a function of the threshold voltage (in volts) applied to the MPPC signal.

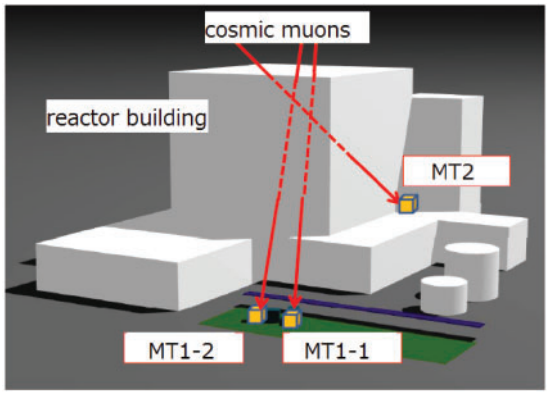

Fig. 5. Locations of the muon telescopes (marked as orange cubes) deployed at the JAPC nuclear power reactor.

operational. When it is not operational, the fuel is usually moved to the NFSP adjacent to the reactor core. MT2 was placed on the roof of a building adjacent to the reactor building, about 30 m away from the reactor center at an elevation of about 10 m from ground level.

The data recording in this detector configuration started in February 2013. Combining the images obtained by MT1 at MT1-1 and MT1-2, and MT2, we constructed a three-dimensional image of the nuclear fuel assemblies stored in the NFSP. The numbers of events used for the analysis were about 15 million at MT1-1, 12 million at MT1-2, and 8 million at MT2.

3.2. Two-dimensional Images of the reactor

From the cosmic muon distributions observed at the three detector positions, we reconstructed the inner structure of the reactor. This reconstruction of the reactor structure involved the following steps:

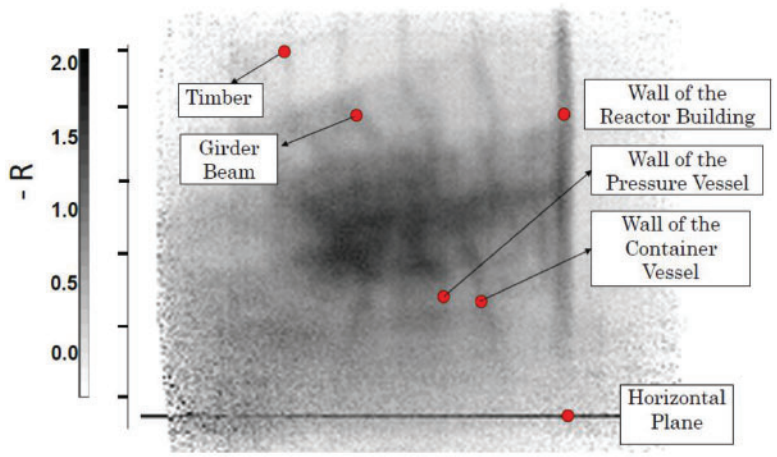

Fig. 6. Image of the reactor complex obtained from 15 million muons observed at MT1-1. The darkness, corresponding to the magnitude of the attenuation of the muon flux, is defined in the text.

1) The "detector direction" is defined as the direction connecting the centers of the two X–Y units in an MT. As we have four X–Y units in MT1 (two of them are in front of the magnet and the other two are behind [3]), we define the detector direction using the front X–Y unit pair only.
2) We define the "image plane" to be perpendicular to the detector direction at the position of the X–Y unit in the rear.
3) We draw the lines of incoming cosmic rays from the hit pos tions recorded by the X–Y unit pair. Then, we calculate the direction $\tan(\theta_x)$ ($\tan(\theta_y)$) of the line determined by the horizontal (vertical) coordinate difference of the two hit positions divided by the spacing of the two. (Note that we allow only one cluster hit in each X–Y unit and therefore only one single line can be reconstructed.) We then calculate the position where this line traverses the image plane. By going through this procedure for all observed muons, we can depict an "image of the reactor" projected on the image plane.
4) We obtain the image of the reactor for each data item obtained at MT1-1, MT1-2, and MT2.

Figure 6 shows an image of the reactor obtained by MT1 at the position MT1-1. The acceptance-corrected event rate is shown by the degree of darkness. The darkenss scale, indicated in the figure, is defined as the negative of the logalithm of the ratio R of the number of observed muons to that expected for a given zenith angle θ and azimuthal angle ϕ,

$$-\ln R = -\ln[N_{\rm obs}(\theta,\phi)/N_{\rm exp}(\theta,\phi)], \tag{1}$$

where the expected number of muons $N_{exp}(\theta\phi)$ is the number of cosmic muons when there are no obstructing materials in the paths of the incoming muons. More details are given in Sect. 3. 3. The darker the spot is, the lower the event rate. The azimuthal angle at the center of the image is about 25˚, while the detector's azimuthal angular coverage is from 0˚ to 40˚.

The pressure vessel, containment vessel, some timbers, and girder beams of the reactor building and the wall of the building are marked by red points in the figure. Note that the horizontal girder beams are quite tilted in the image. One notices that there is no heavy object corresponding to the nuclear fuel at the loading zone in the pressure vessel. The dark region to the left of the containment vessel can be attributed to the NFSP.

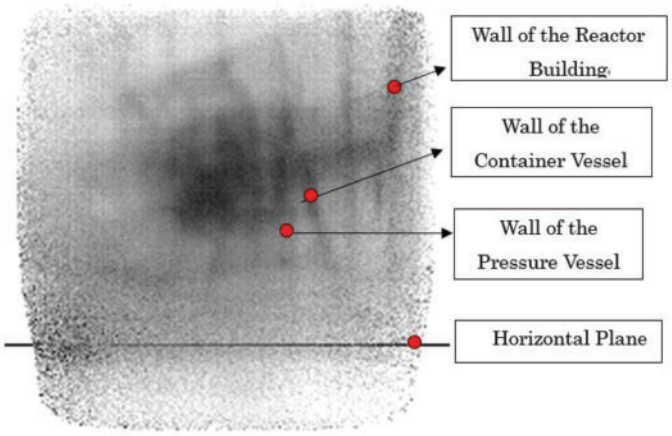

Fig. 7. Image of the reactor complex viewed by MT1 at position MT1-2 The darkness of the image is given in the same units as in Fig. 6.

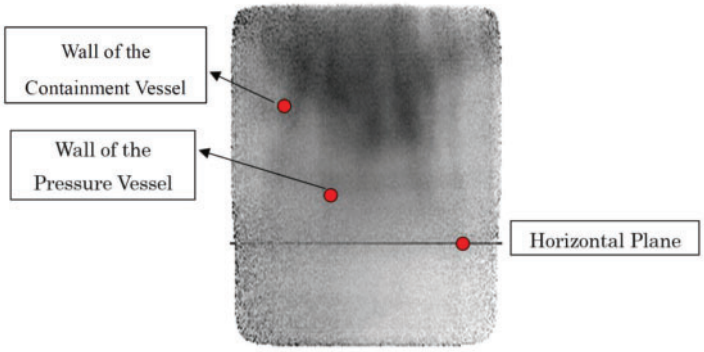

Fig. 8. Image of the reactor complex viewed by MT2. The darkness of the image is given in the same units as in Fig. 6.

Figure 7 shows a similar image obtained by MT1 at position MT1-2. Figure 8 is a similar image obtained by MT2. The NFSP is seen behind the containment vessel.

Figure 9 shows the angular acceptance at MT1-1. MT-1 covers the region from -10˚ to +45˚ in θ and -30˚ to +30˚ in ϕu The image gets blured at shallow θ angles partly because the cosmic muon flux decreases, especially in the low-momentum component which is essential in muon radiography. Figure 10 shows the angular coverage viewed by MT2. It has a similar angular coverage to MT-1 with slightly smaller coverage in θ.

3.3. Three-dimensional image of heavy objects in the NFSP

In order to obtain a three-dimentional image combining the three two-dimensional images, we normalize the observed numbers of muons $N_{obs}(\theta$sg$\phi)$ for given angles of θ andgϕ by dividing them by the expected numbers of muons.

The expected number of muons, $N_{exp}(\theta$sg$\phi)$, is given by the following equation:

$$N_{\rm exp}(\theta,\phi) = F(\theta)\Delta S\Delta\Omega T, \tag{2}$$

where $F(\theta)$ is the cosmic ray flux given as a function of the zenith angle as $F(\theta) = A[(1-r)\cos^2\theta + r]$ with $A = 60$ and $r = 0.025$. ΔS is the effective detection area, $\Delta\Omega$ is the solid angle for detecting

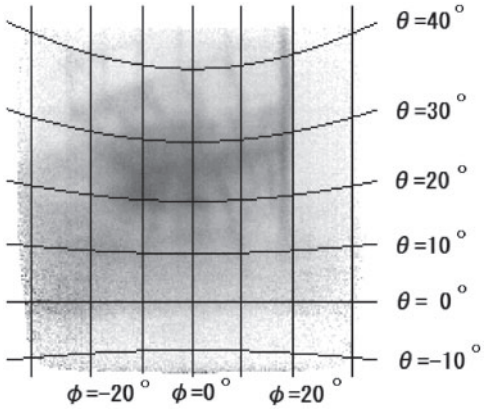

Fig. 9. Angular coverage of the image of the reactor viewed at MT1-1.

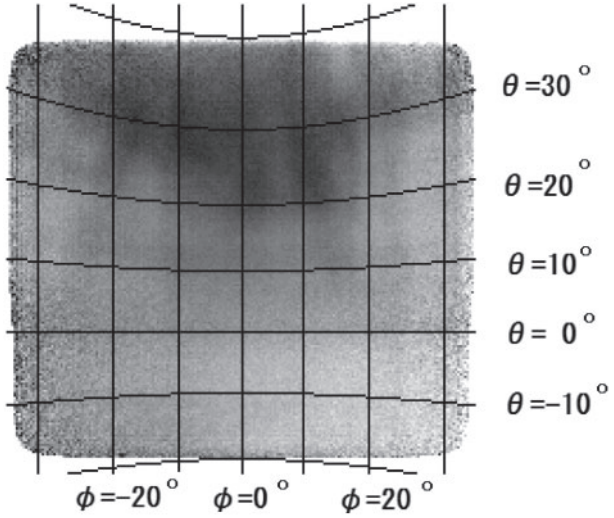

Fig. 10. Angular coverage of the image of the reactor viewed by MT2.

muons, and T is the data-taking time. $F(\theta)$ is given in units of 1 str^{-1} m^{-2} s^{-1}. Here we assume that there is no azimuthal angle dependence of the cosmic ray flux such as an east–west dependence. This formula for the cosmic ray flux was verified using the cosmic ray flux measured with the MT1 at KEK, where the MT1 was placed on the ground with no heavy objects surrounding it. Figure 11 shows the measured cosmic muon flux in black dots as a function of the zenith angle θ, compared with the fomula, $F(\theta)$, shown by the blue solid curve. One sees that the calculated flux, $N_{exp}(\theta \mathrm{sg} \phi)$, reproduces the general features of the observed data, although there is some discepancy. This discrepancy, however, is in the large-θgange and does not distort the imaging of the NFSP region. We note that this formula is consistent with the description given in the Particle Data Book [8].

As we have confirmed [6] that the present muon radiography system can image the inner structure of the reactor building from outside the building, our next step is to locate the nuclear fuel materials stored in the NFSP and obtain their shape three-dimensionally. The starting point is to look for spots of large suppression in the muon flux in the two-dimensional images. To search for an area of significant suppression, we calculate the ratio of the numbers of observed cosmic muons to those expected, $R = N_{obs}(\theta\phi)/N_{exp}(\theta\phi)$. Then, we mark those points as "highly suppressed" when the $\ln R$ values are smaller than the threshold values. The thresholds are set for the three two-dimensional

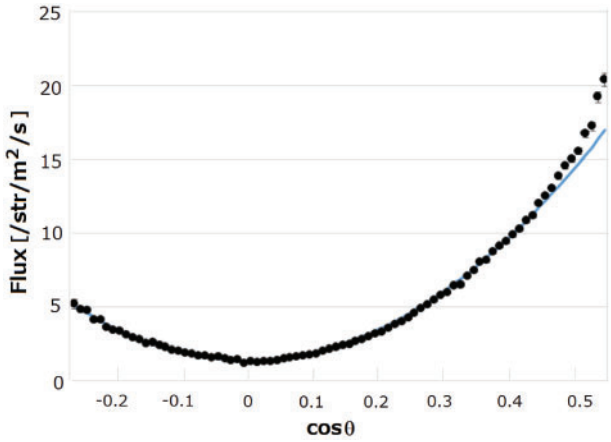

Fig. 11. Observed cosmic ray flux as a function of azimuthal angle with no obstacle material along the muon path. The solid blue curve is a calculation using $F(\theta)$.

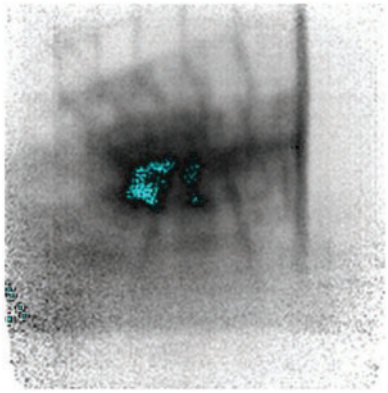

Fig. 12. Spots of significant cosmic ray suppression, $\ln(R) < -1.4$ marked in blue superimposed on the image of Fig. 6.

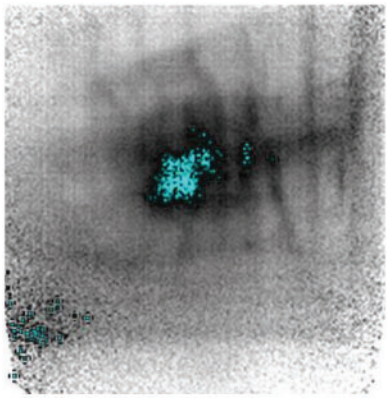

Fig. 13. Spots of significant cosmic ray suppression, marked in blue superimposed on the image of Fig. 7.

images at MT1-1, MT1-2, and MT2 at -1. 4, -1. 5, and -1. 8, respectively. We then mark those "highly suppressed" points as shown in Figs. 12, 13, and 14 in blue points. We observe a concentration of highly suppressed spots at the upper left side of the containment vessel in Figs. 12 and 13, and at the upper part of the containment vessel in Fig. 14, where the NFSP is located.

Fig. 14. Spots of significant cosmic ray suppression, marked in blue superimposed on the image of Fig. 8.

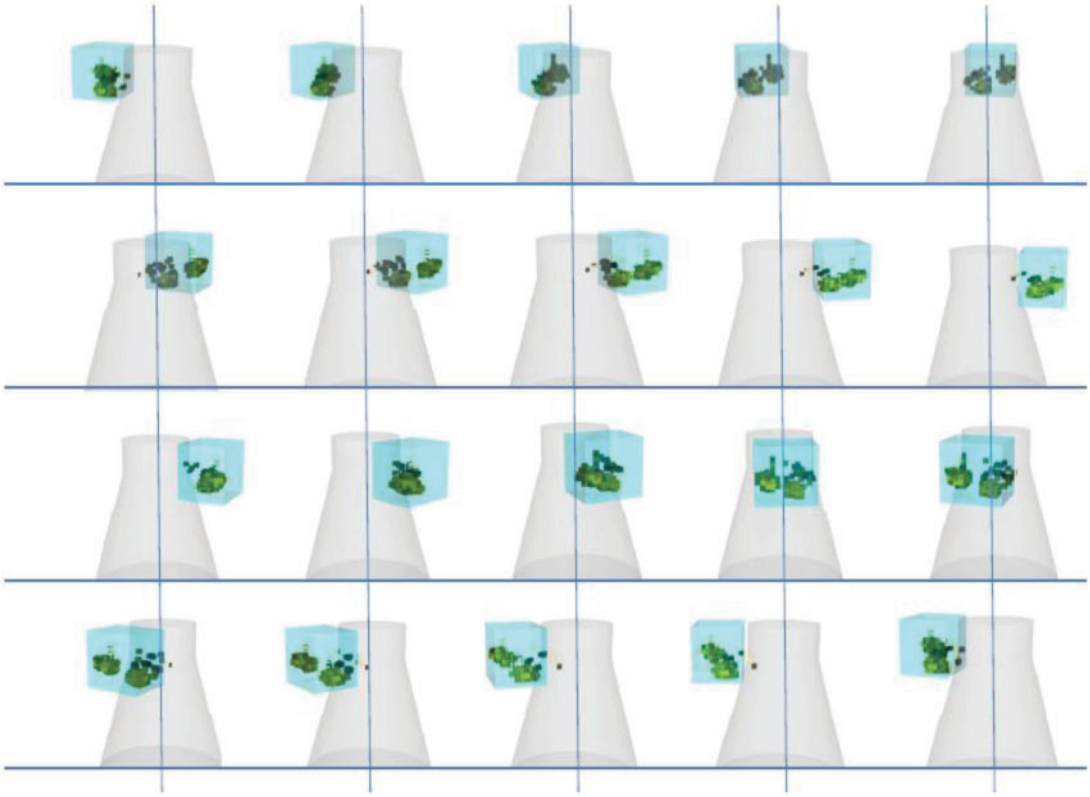

Fig. 15. Reconstructed three-dimensional images of the spots of significant suppression of cosmic muon flux. The images are shown at different view angles varied in steps of 18°. The gray cone shape is the containment vessel and the blue cubic area is the NFSP.

In order to obtain a three-dimensional image of the highly suppressed spots, the NFSP volume is divided into blocks of 1 m^3, and we assign the blocks to be "heavy" if two or three out of the three two-dimensional images of highly suppressed spots point to the same block. The reconstructed shape is displayed in a green color in Fig. 15 together with the water in the NFSP in blue, viewed at 20 different angles around the center axis of the containment vessel. We observe two clusters of heavy blocks in the NFSP. We show one of the 20 images at a magnified scale in Fig. 16. It could be speculated that one cluster is of the spent nuclear fuels and the other of the fuel assemblies to

Fig. 16. One of the images of spots of high absorption.

be used for power generation. We have thus successfully located and obtained a three-dimensional image of the fuel.

3.4. Evaluation of the mass of the heavy object in the NFSP

Evaluation of the mass of the heavy object is the ultimate subject of the muon radiography. Since we have identified the shape of the heavy cluster, the average density is the quantity to be derived. The property that the muon absorption in a material is dependent on the density times the path length of the muons (density-length) is used to derive the average density. However, the absorption is also dependent on the muon momentum, and the muon energy spectrum becomes harder at lower zenith angles [8], which needs to be taken into account.

The zenith angle dependence of the muon absorption to density-length relation was derived using the measured muon transmittance data through the containment vessel, the pressure vessel, and other reactor building materials, but excluding the area of the NFSP. The density-length along such objects was calculated from the known materials and dimensions. Figure 17 shows the calculated density-length distribution viewed by MT2.

The muon transmittance, T_m, is found to be approximated well by the following equation:

$$-\ln(T_{\mathrm{m}}) = a(\theta)\sqrt{L_{\mathrm{D}}}, \tag{3}$$

where L_D is the density-length, and $a(\theta)$ is the zenith-angle-dependent coefficient. Figure 18 shows an example of the relation between the muon transmittance and the density-length viewed by MT2 at $\theta = 67.2°$. We found that the relation can be approximated well by this formula. Figure 19 plots the coefficient $a(\theta)$ as a function of the zenith angle.

Figure 20 shows the density-length distribution observed by MT2 derived from Eq. (3) using the measured muon transmittance and the coefficient $a(\theta)$. The upper plot shows the distribution in the entire view area. The lower plot is the density-length distribution inside the NFSP where the density-length of the objects outside the NFSP is subtracted from the top plot.

The final procedure is the evaluation of the average density of the heavy object clusters shown in Fig. 16. We assume that both clusters are rectangular and located in the NFSP, as shown in Fig. 21.

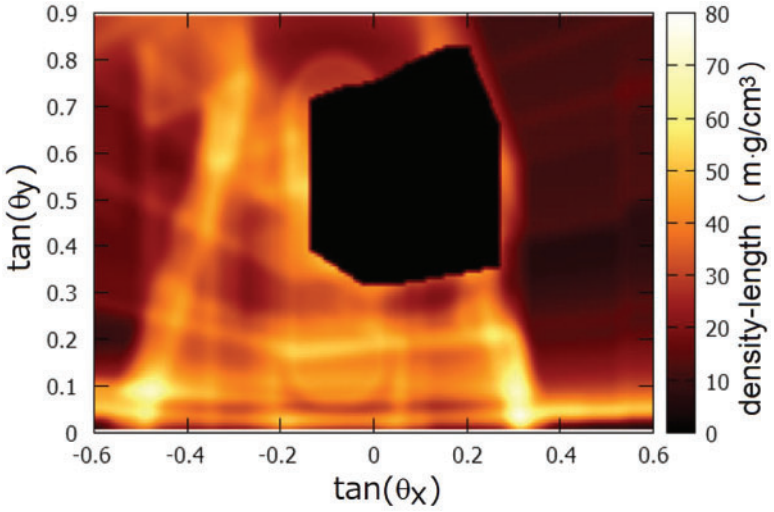

Fig. 17. Density-length distribution seen by MT2 calculated using known density and dimension values. The coordinates are the horizontal and vertical directions (see Sect. 3. 2) of MT2. The area corresponding to the NFSP (black) is excluded in this calculation.

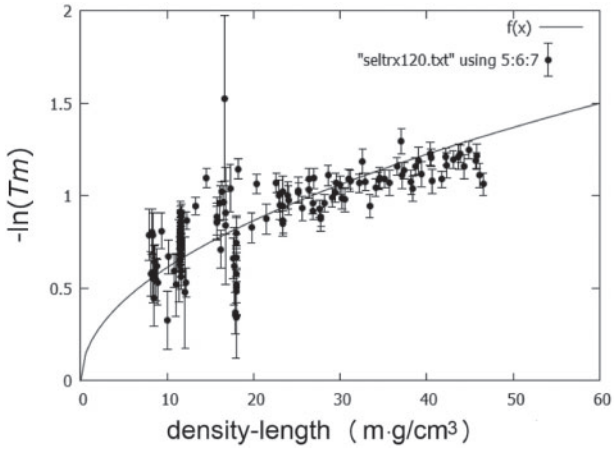

Fig. 18. Relationship between the calculated density-length and the measured muon transmittance at $\theta = 67.2°$. The curve is a fit to the formula in Eq. (3).

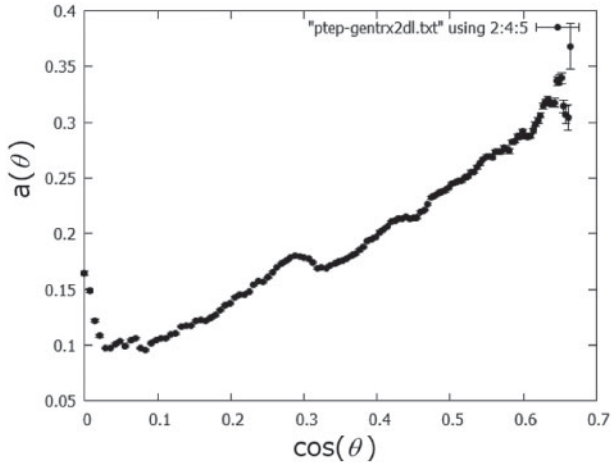

Fig. 19. The coefficient $a(\theta)$ obtained from the measured muon transmittance and the density-length distributions calculated for known objects in the region excluding the NFSP.

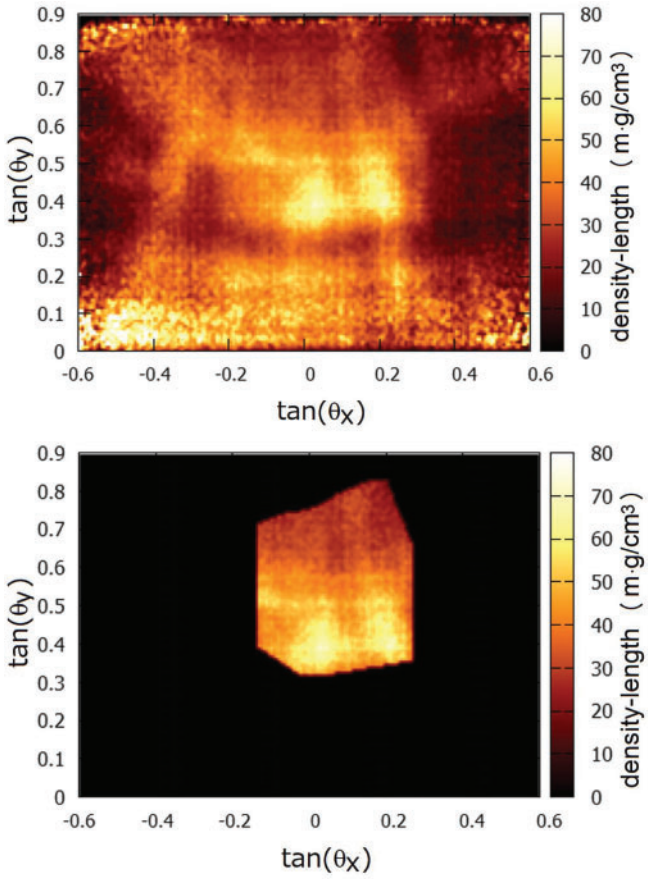

Fig. 20. The density-length distributions estimated from the MT2 data: (top) in the entire view area; (bottom) inside the NFSP.

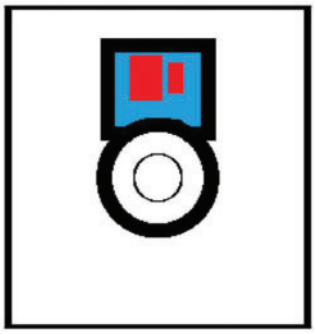

Fig. 21. Assumed cross-sectional view of the reactor at the height of the NFSP, showing the rectangular reactor building wall, the circular containment and pressure vessels, and the NFSP (water in blue). The locations and sizes of the observed heavy objects (red squares) are to be adjusted to reproduce the measured data.

Figure 22 shows the obtained density-length distribution inside the NFSP as a function of horizontal direction $\tan(\theta_x)$ in comparison with the estimates, varying the average density of the heavy clusters at $\theta \sim 68°$. Note that θ is not constant as $\tan(\theta_y)$ is fixed in this plot—see Fig. 10. The comparison in the entire NFSP region results in the following optimum sizes and density for the two heavy objects:

- Cluster 1 (left rectangle in Fig. 21):
  4.5 m (left to right) × 6. 5 m (top to bottom) and 4 m in height.

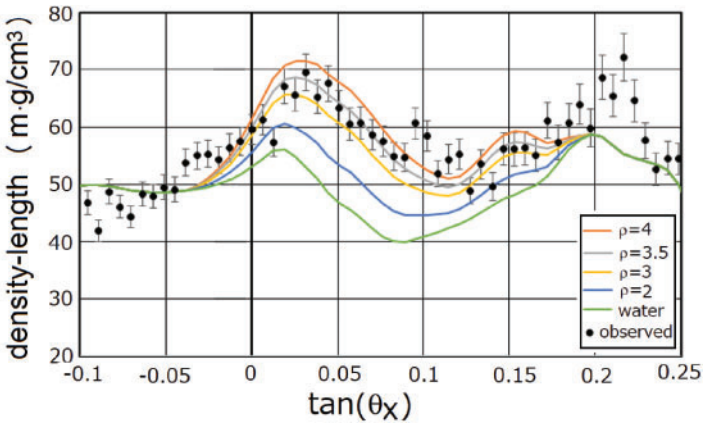

Fig. 22. The density-length distribution inside the NFSP compared with estimates using various densities, ρ, of the heavy object clusters.

- Cluster 2 (right rectangle in Fig. 21):
  3 m (left to right) $\times$ 5. 4 m (top to bottom) and 4 m in height.
- Average density (common for both): 3. 5 $\pm$ 0. 5 g cm^{-3}.

Therefore, the weights of the heavy clusters are:

- Cluster 1: 410 $\pm$ 60 tons
- Cluster 2: 227 $\pm$ 35 tons
- Total: 637 $\pm$ 95 tons

For a typical water occupation of 65% in volume, the above weight refers to a net weight of 519 tons for the fuel assemblies alone and a density of 2. 8 g cm^{-3} excluding the water. This corresponds to 2000–2100 fuel assemblies located in the NFSP for a typical unit weight of 250 kg.

In the previous paper [3], we estimated using the MT1-1 data that an (unseparated) fuel cluster extended 6 m from top to bottom (see Fig. 21) and 7 m from left to right (Fig. 21) under the assumption of an average density of 2. 5 g cm^{-3}. Since the clusters viewed from MT-1 are not separated, the previous observation is consistent with the present estimates. Also, the assumed density of 2. 5 g cm^{-3} is consistent with 2. 8 g cm^{-3} when taking the uncertainty into account.

4. Conclusions

We investigated the inner structure of the nuclear reactor at JAPC, Tokai, Ibaraki, Japan, with a muon radiography system by using cosmic muons. The detectors were placed outside the reactor building. We succeeded in observing the containment vessel, pressure vessel, and other components of the reactor building. From the three views, we also succeeded in locating two heavy object clusters which are considered to be the nuclear fuel assemblies stored in the nuclear fuel storage pool. The mass of the fuel assemblies was derived using density-length measurements.

Acknowledgements

We thank the Japan Atomic Power Company (JAPC) for undertstanding the importance of this study, and for their cooperation and support in carrying out this project. We thank Professor Hirotaka Sugawara of the Okinawa Institute of Science and Technology for his advice and suggestions.

References

[1] K. Nagamine, M. Iwasaki, K. Shimomura, and K. Ishida, Nucl. Instrum. Meth. A **356**, 585 (1995).
[2] H. Tanaka, K. Nagamine, N. Kawamura, S. N. Nakamura, K. Ishida, and K. Shimomura, Hyperfine Interact. **138**, 521 (2001).
[3] H. Fujii et al., Prog. Theor. Exp. Phys. **2013**, 073C01 (2013).
[4] A. Pla-Dalmau, A. D. Bross, and K. L. Mellott, Nucl. Instrum. Meth. A **466**, 482 (2001).
[5] Kuraray Co. Ltd.
[6] Hamamatsu Photonics Ltd.
[7] K. Takahashi, Senior Thesis, University of Tsukuba (2014).
[8] J. Beringer et al. [Particle Data Group], Phys. Rev. D **86**, 010001 (2012).